Corrective $N-k$ Security-constrained Unit Commitment Using Lossy Shift Factors and Fictitious Injections

Sergio Ramírez-López, Guillermo Gutiérrez-Alcaraz, *Senior Member*, *IEEE*, José M. Arroyo, *Fellow*, *IEEE*, and Víctor H. Hinojosa, *Member*, *IEEE*

***Abstract*—Power systems worldwide are increasingly experiencing the simultaneous failure of multiple components due to severe weather conditions, which are becoming more frequent and intense. This consequently triggers growing interest in more stringent security standards. Indeed, electricity markets are moving toward explicitly including generator outages within auction models seeking the most economical and reliable generation scheduling and dispatch. Within this context, a corrective $N-k$ security-constrained unit commitment model is proposed to address the need for tighter security standards. As a major distinctive feature, the proposed model jointly considers multiple out-of-service generators and lines, corrective actions, and transmission line losses. Moreover, unlike previous studies, lossy shift factors are used to represent the effect of the lossy transmission network while accurately characterizing transmission line losses by a binary-variable-based piecewise linear approximation. Additionally, line outages are incorporated by modeling fictitious injections of active power. The proposed model using lossy shift factors and fictitious injections is cast as an instance of mixed-integer linear programming. The solution of the resulting mathematical problem allows co-optimizing energy and reserves to accommodate the power fluctuations due to the component outages under consideration. Numerical experience is reported using three standard benchmarks comprising 14, 118, and 500 buses.**

***Index Terms*—Unit commitment, $N-k$ security criterion, generator outage, line outage, lossy shift factor, transmission line loss, fictitious injection.**

Manuscript received: May 15, 2025; revised: August 5, 2025; accepted: December 5, 2025. Date of CrossCheck: December 5, 2025. Date of online publication: January 16, 2026.

The work of S. Ramírez-López was supported by the SECIHTI (No. 1142853) under the Programa de Graduados e Investigación en Ingeniería Eléctrica (PGIIE), Tecnológico Nacional de México/Instituto Tecnológico de Morelia (ITM). The work of G. Gutiérrez-Alcaraz was supported by the PRODEP (No. 8127/ITMOR-CA-6). The work of J. M. Arroyo was supported by the EU Horizon Europe Programme (No. 101160614), the MSCA Doctoral Network (No. 101168796), MICIN/MICIU/AEI and ERDF (No. PID2021-122579OB-I00, PID2021-126566OB-I00, PID2024-159031OB-I00), Junta de Comunidades de Castilla-La Mancha and ERDF (No. SBPLY/21/180501/000154), and the Universidad de Castilla-La Mancha (No. 2025-GRIN-38264).

S. Ramírez-López and G. Gutiérrez-Alcaraz (corresponding author) are with Tecnológico Nacional de México/Instituto Tecnológico de Morelia (ITM), Morelia 58120, Mexico (e-mail: D16121518@morelia.tecnm.mx; guillermo.ga@morelia.tecnm.mx).

J. M. Arroyo is with the Escuela Técnica Superior de Ingeniería Industrial, Universidad de Castilla-La Mancha, Ciudad Real 13071, Spain (e-mail: joseman-uel.arroyo@uclm.es).

V. H. Hinojosa is with the Department of Electrical Engineering, Universidad Técnica Federico Santa María, Valparaíso 23901223, Chile (e-mail: victor.hinojosa@usm.cl).

DOI: 10.35833/MPCE.2025.000430

NOMENCLATURE

A. Constants

$\zeta_{s,l}$	Parameter of linearized line loss function
B_l, G_l	Line susceptance and conductance
$C_{i,t}^{Dn}$, $C_{i,t}^{Up}$	Offer cost rates for downward and upward spinning reserve contributions
$C_{j,t}^{ENS}$	Nodal load shedding cost coefficient
$C_{i,t}^{SD}$, $C_{i,t}^{SU}$	Cost coefficients for shutdowns and start-ups
DT_i, UT_i	Minimum down and up time
$F_l^{\max}$	Line active power flow capacity
$fr(l)$, $to(l)$	Sending and receiving buses
$P_{j,t}^d$	Nodal load demand
$P_i^{g,\max}$, $P_i^{g,\min}$	Maximum and minimum power generation limits
RD_i, RU_i	Downward and upward ramping limitations
$R_i^{\max,Dn}$, $R_i^{\max,Up}$	Upper bounds for downward and upward spinning reserve contributions
SD_i, SU_i	Ramping limitations for shutdowns and start-ups
$SF_{l,j}^{loss}$	Lossy shift factor
$T_{i,0}^{DT}$, $T_{i,0}^{UT}$	Durations of initial offline and online intervals associated with minimum down time and minimum up time
$T_{i,0}^{off}$, $T_{i,0}^{on}$	Durations of initial offline and online states
$U_{i,0}$	Initial commitment state (1 for online, 0 otherwise)

B. Functions

$C_{i,t}^P(\cdot)$	Production cost offer

C. Variables

$\Delta\hat{f}_{s,l,t}$, $\Delta\hat{f}_{s,l,t}^c$	Variables of linearized line loss functions in pre-contingency state and under contingency
$cd_{i,t}$, $cu_{i,t}$	Shutdown and start-up costs
$ens_{j,t}$, $ens_{j,t}^c$	Pre- and post-contingency nodal load shedding
$f_{l,t}^{loss}$, $f_{l,t}^{loss,c}$	Pre- and post-contingency active power line

	losses
$\hat{f}_{l,t}, \hat{f}_{l,t}^{c}$	Auxiliary variables of pre- and post-contingency power flow models
$\hat{f}_{l,t}^{+}, \hat{f}_{l,t}^{-}$	Auxiliary variables used to model the absolute value of $\hat{f}_{l,t}$
$\hat{f}_{l,t}^{+,c}, \hat{f}_{l,t}^{-,c}$	Auxiliary variables used to model the absolute value of $\hat{f}_{l,t}^{c}$
$p_{i,t}^{g}, p_{i,t}^{g,c}$	Pre- and post-contingency active power outputs
$r_{i,t}^{Dn}, r_{i,t}^{Up}$	Downward and upward spinning reserve contributions
$u_{i,t}$	Binary variable for generation scheduling (1 for online, and 0 otherwise)
$y_{l,t}, y_{l,t}^{c}$	Binary variables used to impose the complementarity condition in the linearized functions for pre- and post-contingency line losses
$z_{s,l,t}, z_{s,l,t}^{c}$	Binary variables used to impose the adjacency condition in the linearized functions for pre- and post-contingency line losses

D. Sets

I	Set of indices i for generators
I_j	Set of indices i for generators at bus j
I^c	Set of indices i for operational generators under contingency
I_j^c	Set of indices i for generators at bus j that are operational under contingency
$I^{c,n}$	Set of indices i for generators in islanded area n that are operational under contingency
J	Set of indices j for buses
$J^{c,n}$	Set of indices j for buses in islanded area n under contingency
L	Set of indices l and l' for operational transmission lines in the pre-contingency state
L^c	Set of indices l and l' for operational transmission lines under contingency
$L^{c,n}$	Set of indices l for lines in islanded area n that are operational under contingency
N^c	Set of indices n for islanded areas under contingency
S	Set of indices s for blocks of linearized line loss functions
T	Set of indices t and t' for time periods

E. Matrices and Vectors

$\boldsymbol{\Theta}$	Vector of nodal voltage phase angles
$\boldsymbol{\Theta}_r$	Reduced vector of $\boldsymbol{\Theta}$
$\boldsymbol{A}, \bar{\boldsymbol{A}}$	Oriented and unoriented bus-branch incidence matrices
$\bar{\boldsymbol{A}}_r$	Reduced matrix of $\bar{\boldsymbol{A}}$
$\boldsymbol{B}$	Susceptance matrix
$\boldsymbol{B}_d, \boldsymbol{G}_d$	Diagonal matrices of branch series susceptances and conductances
$\boldsymbol{B}_r$	Reduced matrix of $\boldsymbol{B}$
$\hat{\boldsymbol{f}}$	Vector of terms relating line power flows to nodal voltage phase angles
$\boldsymbol{f}^{loss}$	Vector of line losses
$\boldsymbol{F}^{\max}$	Vector of line capacities
$\boldsymbol{M}$	Expanded matrix of $\boldsymbol{B}_r^{-1}$
$\boldsymbol{P}^d$	Vector of nodal demands
$\boldsymbol{P}_r^d$	Reduced vector of $\boldsymbol{P}^d$
$\boldsymbol{p}^g$	Vector of nodal generations
$\boldsymbol{p}_r^g$	Reduced vector of $\boldsymbol{p}^g$
$\boldsymbol{SF}^{loss}$	Matrix of lossy shift factors

I. Introduction

NOWADAYS, security-constrained unit commitment (SCUC) and security-constrained economic dispatch models in day-ahead electricity markets have incorporated $N-1$ transmission line outage constraints in their contingency modeling [1]. However, multiple line contingencies are becoming more frequent and severe with the growing penetration of renewable energy generation and increasingly extreme weather conditions [2]-[5]. A relevant example is the largest blackout ever in Turkey in March 2015, affecting about 75 million people due to the outages of multiple transmission lines [6]. Another example occurred in Continental Europe, whose synchronous area was recently separated into two parts due to several out-of-service transmission network elements [7].

Moreover, blackouts may be triggered by not only transmission line outages but also generator contingencies. An example is the blackout in Mumbai, India, in 2020, wherein multiple outages of generators and lines were involved [8]. Consequently, electricity markets are moving toward explicitly including generator outages within auction models, seeking the most economical and reliable generation scheduling and dispatch. For instance, a recent design change in the California Independent System Operator (CAISO) market in the has USA incorporated both generation outages and remedial action schemes [1]. Similarly, the deployment of reserves is specifically characterized in the SCUC formulation run by the Midcontinent Independent System Operator (MISO) in the USA to enhance the co-optimization of energy and ancillary services [9].

The consideration of contingencies accounts for three practical factors in actual power system operation: ① not all transmission line outages result in a contingency alert condition; ② not all generator contingencies affect the system with the same severity; and ③ market-clearing time requirements and current computing capabilities prevent from considering a large number of contingency scenarios, let alone all outages associated with the prescribed security criterion [10]. Thus, a set of pre-defined credible contingencies is typically considered to yield a computationally tractable optimization problem [11]. For instance, based on engineering analysis and outage studies, MISO has developed a procedure to identify over 500 relevant transmission line constraints [10]. Likewise, the market model of MISO accounts for the outage of the largest generator in each zone and the associated post-contingency system reaction [9].

Such industry practice reveals that increasing attention is being paid to more complex generation scheduling instances, particularly models considering multiple simultaneous outages wherein preventive and corrective security actions ensure the feasibility of power system operation. Preventive models enforce the security constraints corresponding to transmission outages so that a common schedule and dispatch for all system states yields no violations under any credible contingency [12]. By contrast, corrective actions under contingency include redispatching generators and curtailing selected loads, which adds flexibility to the power system operation [13], [14]. Therefore, corrective SCUC (CSCUC), albeit being more complex than preventive SCUC, ensures a better balance between cost and security.

From an academic perspective, various relevant approaches are available in the literature on CSCUC. In [15] and [16], a stochastic SCUC model addresses market clearing by considering a pre-specified set of credible contingencies and their probability of occurrence. In [17], the formulation described in [15] is adapted for the day-ahead scheduling of generation, consumption, and spinning reserves. Generation scheduling under a deterministic $N-k$ security criterion is modeled in [14] and [18] using robust optimization, which allows for representing all possible component outages in an implicit fashion.

A modified version of the $N-k$ security standard, referred to as the $N-k-\varepsilon$ criterion, is addressed in [19]. The resulting CSCUC instance is solved by a particularly tailored cutting plane algorithm that prevents from explicitly modeling the power system operation under an exponential number of contingencies. A CSCUC model with a deterministic $N-1-1$ security criterion is presented in [20]. This variant involves the sequential outage of two components, namely generators and/or transmission lines, while considering some time for the reaction against the first outage and pre-positioning against the second outage.

With the increasing penetration of renewable energy generation, alternative approaches jointly accounting for component outages and uncertainty have been reported. In [21], robust optimization is proposed for scheduling quick-start generators while considering an $N-k$ security criterion and various types of uncertainty. An adjustable robust model is presented in [22] to ensure the deliverability of reserves under wind uncertainty and system component outages. Interestingly, the CSCUC model reported in [23] jointly considers generator and transmission line outages under a deterministic $N-1$ security criterion, chance-constrained stochastic programming to model the impact of wind on security, and the co-optimization of generation reserves to handle both wind power fluctuations and out-of-service components. In the robust model proposed in [24], the outage probabilities of generators and transmission lines are incorporated into the uncertainty set modeling. In [25], a robust formulation is presented considering the same security criterion adopted in [20] and renewables-based generation. To address the complexity caused by the penetration of renewable energy generation, the formulation results in an extremely large adaptive robust mixed-integer linear programming (MILP) model.

Unfortunately, relevant studies in [13]-[25] feature important modeling and methodological issues. It is worth highlighting that all existing studies adopt a direct current (DC) power flow [26]. However, rather than considering the more efficient angle-free industry standard [27], [28], existing studies are based on the classic $B\theta$ formulation, which may be computationally more expensive due to its reliance on bus voltage phase angles. This drawback becomes relevant when power system operation under contingency is explicitly characterized [13], [15]-[17], [19], [20], [23], [25], as the extremely large number of constraints and variables would give rise to intractability even for moderately sized systems. As for those approaches implicitly modeling post-contingency operation [14], [18], [21], [22], [24], the resulting robust models involve three challenging hierarchically nested optimization levels, which are typically addressed by either inexact or computationally inefficient approaches. Note also that all such relevant studies [13]-[25] neglect an important practical aspect, namely transmission losses, thus being potentially prone to suboptimality or even infeasibility.

Motivated by such limitations and the needs of the power industry, this paper proposes a corrective $N-k$ SCUC model, where multiple generator and line outages are considered along with corrective actions and transmission losses. In order to incorporate the $N-k$ security criterion, critical components are identified by extending the outage selection procedure described in [12], which solely focuses on out-of-service transmission assets.

The proposed model features several novel aspects compared with [13]-[25]. The main novelty lies in the increased accuracy of transmission network operation through the consideration of both pre- and post-contingency line losses. It is worth mentioning that, within the context of state-of-the-art approaches, including those based on robust optimization and chance-constrained programming, the nonconvexity of transmission losses would drastically increase the mathematical complexity of the resulting optimization problems, thereby disabling the straightforward application of the solution techniques successfully applied to the previously reported lossless counterparts.

To incorporate losses into CSCUC, the proposed model relies on the lossy DC power flow models presented in [29] and [30], which are enhanced by including binary variables in the piecewise linear approximation of losses. Unlike alternative models for transmission losses customarily used within the DC power flow [31]-[33], three main advantages are featured. Firstly, the effect of losses on the power flows at the sending and receiving ends of each line is explicitly modeled, which is relevant to properly characterize line capacities and nodal power balances. Secondly, no nodal loss allocation factors are required, which is important for practical implementation within a market setting, bearing in mind that the nonlinear nature of line losses precludes the existence of a unique loss allocation scheme. Thirdly, the linearization of line losses does not rely on a base solution. This advantage is especially significant in unit-commitment-based models, wherein generation scheduling decisions may substantially vary across time.

Moreover, different from [29] and [30], the proposed mixed-integer linear formulation of lossy power flow is based on a novel set of shift factors (SFs), which are analogous to the DC SFs commonly used in the power industry [34]. Consequently, unlike the lossy power flow models described in [29] and [30] and the classic $B\theta$ lossless formulation adopted in [13]-[25], transmission losses are explicitly accounted for without involving bus voltage phase angles. Compared with the angle-based counterpart, the proposed model is equivalent in terms of solution quality while requiring fewer variables and equations as voltage phase angles are dropped. The latter aspect may be particularly beneficial from a computational perspective when discrete decisions such as unit commitment variables come into play and the power system operation under multiple contingencies is modeled [27], [28]. Note that, within such a context, the challenges posed by the use of the exact full alternating current (AC) power flow model are yet unresolved. Therefore, the proposed model represents a relevant trade-off between accuracy and computational performance.

Admittedly, the straightforward application of the proposed model to represent contingency power flows and $N-k$ security constraints would still be computationally demanding, as each contingency state is associated with the corresponding SF matrix. Note also that, for contingency states leading to network islanding, SF matrices as many as islanded areas should be computed [35]. Alternatively, as an additional distinctive aspect over [13]-[25], this paper effectively and equivalently incorporates transmission contingency constraints into the CSCUC problem by modeling fictitious injections of active power [26]. To that end, we extend the scope of [36] and [37] to a loss-concerned framework. The inclusion of fictitious injections is computationally attractive as the characterization of power flows under contingency solely requires the computation of the pre-contingency SFs irrespective of the system components that are out of service [36], [37] or whether outages give rise to network islanding. Thus, a single SF matrix is involved so that the proposed model efficiently includes corrective actions under contingency, i.e., generation redispatch.

The proposed model using lossy SFs and fictitious injections is a mixed-integer linear program that is solved by the state-of-the-art branch-and-cut algorithm. From a methodological standpoint, two main advantages are featured: ① the well-known properties related to convergence and solution quality, namely guaranteed finite convergence to the optimum while providing a measure of the distance to optimality along the solution process; ② the availability of efficient off-the-shelf software, which is relevant for practical implementation. Moreover, on the modeling side, this paper significantly departs from the closely related studies on corrective $N-k$ SCUC models, as summarized in Supplementary Material A Table SAI. Thus, the findings described hereinafter contribute to knowledge in three main respects:

1) A corrective $N-k$ SCUC model is provided, where $N-k$ generator and transmission outages are considered. Fictitious injections of active power are used to model transmission contingencies, thereby solely requiring the computation of the pre-contingency SF matrix even for contingency states leading to network islanding.

2) A new computationally efficient SF-based power flow is used to include pre- and post-contingency transmission losses. Thus, the resistive effect of transmission lines is adequately characterized.

3) The proposed model guarantees the deployment and delivery of reserves under contingency while accounting for loss-aware power system operation.

The remainder of this paper is organized as follows. Section II describes the computation of lossy SFs. Section III presents the formulation of the proposed model. Section IV reports case studies. Finally, this paper is concluded in Section V, where relevant features are highlighted and future avenues of research are suggested.

II. Computation of Lossy SFs

According to industry practice [34] and relevant studies on CSCUC [13]-[25], power system operation is solely considered at the high-voltage transmission level, and the characterization of the transmission network relies on the widely used DC power flow. Note that the conditions required by the DC power flow [26], [38] hold at the transmission level, i. e., the series resistance of each branch is small compared with its series reactance, the nodal voltage phase angle differences are small, and nodal voltage magnitudes are close to 1 p.u..

Based on [29] and [30], the DC power flow considering losses is formulated using a matrix notation as:

$$\boldsymbol{p}^g-\boldsymbol{P}^d=\boldsymbol{A}\hat{\boldsymbol{f}}+0.5\bar{\boldsymbol{A}}\boldsymbol{f}^{loss} \tag{1}$$

$$\hat{\boldsymbol{f}}=-\boldsymbol{B}_d\boldsymbol{A}^{\mathrm{T}}\boldsymbol{\Theta} \tag{2}$$

$$\boldsymbol{f}^{loss}=\boldsymbol{G}_d\boldsymbol{B}_d^{-2}\hat{\boldsymbol{f}}^2 \tag{3}$$

$$\hat{\boldsymbol{f}}+0.5\boldsymbol{f}^{loss}\leq\boldsymbol{F}^{\max} \tag{4}$$

$$-\hat{\boldsymbol{f}}+0.5\boldsymbol{f}^{loss}\leq\boldsymbol{F}^{\max} \tag{5}$$

where $\boldsymbol{B}_d=\mathrm{diag}\left(B_1,B_2,...,B_{|L|}\right)$ and $\boldsymbol{G}_d=\mathrm{diag}\left(G_1,G_2,...,G_{|L|}\right)$.

Nodal power balance equations are modeled in (1), where the right-hand side accounts for the outgoing line power flows at every bus. The dependence of the power flow model on nodal voltage phase angles is characterized in (2). Line losses are expressed in (3), where $\hat{\boldsymbol{f}}^2$ denotes the entry-wise square of vector $\hat{\boldsymbol{f}}$. Finally, line power flow limits are imposed in (4) and (5), which are associated with the outgoing line power flows at the corresponding sending and receiving buses, respectively.

As described next, the above formulation for the loss-concerned DC power flow can be equivalently recast so that voltage phase angles are dropped and a new set of sensitivity factors, namely lossy SFs, are defined. Using (2) in (1) and rearranging the terms yields:

$$\boldsymbol{p}^g-\boldsymbol{P}^d-0.5\bar{\boldsymbol{A}}\boldsymbol{f}^{loss}=-\boldsymbol{A}\boldsymbol{B}_d\boldsymbol{A}^{\mathrm{T}}\boldsymbol{\Theta}=\boldsymbol{B}\boldsymbol{\Theta} \tag{6}$$

Note that matrix $\boldsymbol{B}$ is singular and $\mathbf{1}^{\mathrm{T}}\boldsymbol{B}=\mathbf{0}^{\mathrm{T}}$, where $\mathbf{1}$ is the all-ones vector and $\mathbf{0}$ is the all-zeros vector. Hence, we have:

$$\mathbf{1}^{\mathrm{T}}\left(\boldsymbol{p}^{g}-\boldsymbol{P}^{d}-0.5\bar{\boldsymbol{A}}\boldsymbol{f}^{loss}\right)=0 \tag{7}$$

By arbitrarily choosing a reference bus for voltage phase angles and arbitrarily selecting a slack bus to ensure power balance, (6) becomes:

$$\boldsymbol{p}_{r}^{g}-\boldsymbol{P}_{r}^{d}-0.5\bar{\boldsymbol{A}}_{r}\boldsymbol{f}^{loss}=\boldsymbol{B}_{r}\boldsymbol{\Theta}_{r} \tag{8}$$

where $\boldsymbol{p}_{r}^{g}$, $\boldsymbol{P}_{r}^{d}$, and $\bar{\boldsymbol{A}}_{r}$ result from removing the row corresponding to the slack bus from $\boldsymbol{p}^{g}$, $\boldsymbol{P}^{d}$, and $\bar{\boldsymbol{A}}$, respectively; $\boldsymbol{\Theta}_{r}$ results from dropping the row corresponding to the reference bus in $\boldsymbol{\Theta}$; and $\boldsymbol{B}_{r}$ results from $\boldsymbol{B}$ without the row corresponding to the slack bus and the column associated with the reference bus.

From (8), we have:

$$\boldsymbol{\Theta}_{r}=\boldsymbol{B}_{r}^{-1}\left(\boldsymbol{p}_{r}^{g}-\boldsymbol{P}_{r}^{d}-0.5\bar{\boldsymbol{A}}_{r}\boldsymbol{f}^{loss}\right) \tag{9}$$

Moreover, the vector of nodal voltage phase angles $\boldsymbol{\Theta}$ can be expressed as:

$$\boldsymbol{\Theta}=\boldsymbol{M}\left(\boldsymbol{p}^{g}-\boldsymbol{P}^{d}-0.5\bar{\boldsymbol{A}}\boldsymbol{f}^{loss}\right) \tag{10}$$

where $\boldsymbol{M}$ results from expanding $\boldsymbol{B}_{r}^{-1}$ with a row of zeros for the reference bus and a column of zeros for the slack bus.

Finally, using (10) in (2) gives rise to:

$$\hat{\boldsymbol{f}}=-\boldsymbol{B}_{d}\boldsymbol{A}^{\mathrm{T}}\boldsymbol{M}\left(\boldsymbol{p}^{g}-\boldsymbol{P}^{d}-0.5\bar{\boldsymbol{A}}\boldsymbol{f}^{loss}\right)=\boldsymbol{SF}^{loss}\cdot\left(\boldsymbol{p}^{g}-\boldsymbol{P}^{d}-0.5\bar{\boldsymbol{A}}\boldsymbol{f}^{loss}\right) \tag{11}$$

where $\boldsymbol{SF}^{loss}=-\boldsymbol{B}_{d}\boldsymbol{A}^{\mathrm{T}}\boldsymbol{M}$.

Thus, the SF-based equivalent to the original loss-concerned DC power flow model (1)-(5) comprises (3)-(5), (7), and (11).

III. Proposed Model

This section formulates the proposed model considering an $N-k$ security criterion, transmission losses, and fictitious injections of active power.

A. Selection of Component Outages

The proposed model relies on the ex-ante selection of critical component outages, which are thus input data for the optimization process. The rationale of this procedure lies in assigning criticality based on the severity of component outages with respect to normal operation under peak load, so that component outages are ranked in descending order of severity. Regarding transmission line outages, their potential impact on security is computed using the approach reported in [12], which has been extended to consider radial lines. As for generators, their criticality is determined according to the base-case dispatch. Those contingency states that are structurally critical due to resource inadequacy, i. e., inability to meet power balance due to insufficient generation or transmission capacity, are discarded since they cannot be handled by appropriately operating the system. As a result, a proxy for quickly identifying potential umbrella contingency states [39] is devised, which is suitable for practical implementation.

Alternative outage selection algorithms may be used, leveraging experience, engineering judgment, and even recent artificial intelligence developments. However, the analysis of the impact of those choices is beyond the scope of this paper.

B. Objective Function and Cost-related Terms

The optimization goal formulated in (12) is the minimization of the total cost, which includes terms related to pre-contingency power generation, start-ups, shutdowns, up-spinning reserves, down-spinning reserves, as well as pre- and post-contingency load shedding:

$$\min\left\{\sum_{t\in T}\sum_{i\in I}\left[C_{i,t}^{P}\left(p_{i,t}^{g},u_{i,t}\right)+cu_{i,t}+cd_{i,t}+C_{i,t}^{Up}r_{i,t}^{Up}+C_{i,t}^{Dn}r_{i,t}^{Dn}\right]+\sum_{t\in T}\sum_{j\in J}\left(C_{j,t}^{ENS}\cdot ens_{j,t}+C_{j,t}^{ENS}\cdot ens_{j,t}^{c}\right)\right\} \tag{12}$$

The start-up costs are modeled in (13) and (14), whereas (15) and (16) are related to shutdown costs:

$$cu_{i,t}\ge C_{i,t}^{SU}\left(u_{i,t}-u_{i,t-1}\right)\quad\forall i\in I,\forall t\in T \tag{13}$$

$$cu_{i,t}\ge 0\quad\forall i\in I,\forall t\in T \tag{14}$$

$$cd_{i,t}\ge C_{i,t}^{SD}\left(u_{i,t-1}-u_{i,t}\right)\quad\forall i\in I,\forall t\in T \tag{15}$$

$$cd_{i,t}\ge 0\quad\forall i\in I,\forall t\in T \tag{16}$$

C. Power Balance

Constraints (17) and (18) represent the pre- and post-contingency system power balance equations, respectively. Following a contingency event, the deployment of spinning reserves modeled by $p_{i,t}^{g,c}$ provides the power required to compensate for generator and/or line outages. To flag the absence of a feasible solution under some operating conditions, power balance equations (17) and (18) include load shedding variables $ens_{j,t}$ and $ens_{j,t}^{c}$, which are bounded in (19) and (20), respectively, and conveniently penalized in the objective function (12). Moreover, network islanding under contingency is accounted for in (18).

$$\sum_{i\in I}p_{i,t}^{g}+\sum_{j\in J}ens_{j,t}=\sum_{j\in J}P_{j,t}^{d}+\sum_{l\in L}f_{l,t}^{loss}\quad\forall t\in T \tag{17}$$

$$\sum_{i\in I^{c,n}}p_{i,t}^{g,c}+\sum_{j\in J^{c,n}}ens_{j,t}^{c}=\sum_{j\in J^{c,n}}P_{j,t}^{d}+\sum_{l\in L^{c,n}}f_{l,t}^{loss,c}\quad\forall t\in T,\forall n\in N^{c} \tag{18}$$

$$0\le ens_{j,t}\le P_{j,t}^{d}\quad\forall j\in J,\forall t\in T \tag{19}$$

$$0\le ens_{j,t}^{c}\le P_{j,t}^{d}\quad\forall j\in J,\forall t\in T \tag{20}$$

D. Operation of Generators

The model for the operation of generators is based on the MILP formulations presented in [13] and [40], which have been widely used in the technical literature and industry practice. Further details on the computational performance of MILP unit-commitment-based models can be found in [41] and references therein.

As per (21)-(23), pre-contingency generation and reserve contributions are bounded by the corresponding production limits for generators scheduled to be on, being equal to 0 for generators scheduled to be off. Constraints (24) and (25) bound the reserve contributions from individual generators. Accordingly, the energy and reserve schedule features the flexibility required to accommodate the power fluctuations under contingency. Post-contingency production is bounded in (26).

Constraint (27) models the relationship among the pre-contingency dispatch, post-contingency dispatch, and up- and down-spinning reserves. In (28), the production of the out-of-service generators in the contingency state is set to be 0. Finally, (29) models the binary generation scheduling variable $u_{i,t}$.

$$P_i^{g,\min} u_{i,t} \le p_{i,t}^g \le P_i^{g,\max} u_{i,t} \quad \forall i \in I, \forall t \in T \tag{21}$$

$$p_{i,t}^g + r_{i,t}^{Up} \le P_i^{g,\max} u_{i,t} \quad \forall i \in I, \forall t \in T \tag{22}$$

$$p_{i,t}^g - r_{i,t}^{Dn} \ge P_i^{g,\min} u_{i,t} \quad \forall i \in I, \forall t \in T \tag{23}$$

$$0 \le r_{i,t}^{Up} \le R_i^{\max, Up} \quad \forall i \in I, \forall t \in T \tag{24}$$

$$0 \le r_{i,t}^{Dn} \le R_i^{\max, Dn} \quad \forall i \in I, \forall t \in T \tag{25}$$

$$P_i^{g,\min} u_{i,t} \le p_{i,t}^{g,c} \le P_i^{g,\max} u_{i,t} \quad \forall i \in I^c, \forall t \in T \tag{26}$$

$$p_{i,t}^g - r_{i,t}^{Dn} \le p_{i,t}^{g,c} \le p_{i,t}^g + r_{i,t}^{Up} \quad \forall i \in I^c, \forall t \in T \tag{27}$$

$$p_{i,t}^{g,c} = 0 \quad \forall i \notin I^c, \forall t \in T \tag{28}$$

$$u_{i,t} \in \{0, 1\} \quad \forall i \in I, \forall t \in T \tag{29}$$

Note that $u_{i,t}$ is used for both the pre-contingency and contingency states, indicating that post-contingency corrective actions can only be provided by generators that are scheduled in the pre-contingency state [13].

Constraints (30) and (31) represent the ramping limits for the pre-contingency state.

$$p_{i,t}^g + r_{i,t}^{Up} - \left(p_{i,t-1}^g - r_{i,t-1}^{Dn}\right) \le RU_i \cdot u_{i,t-1} + SU_i \cdot \left(u_{i,t} - u_{i,t-1}\right) + P_i^{g,\max}\left(1 - u_{i,t}\right) \quad \forall i \in I, \forall t \in T \tag{30}$$

$$p_{i,t-1}^g + r_{i,t-1}^{Up} - \left(p_{i,t}^g - r_{i,t}^{Dn}\right) \le RD_i \cdot u_{i,t} + SD_i \cdot \left(u_{i,t-1} - u_{i,t}\right) + P_i^{g,\max}\left(1 - u_{i,t-1}\right) \quad \forall i \in I, \forall t \in T \tag{31}$$

Additionally, (32)-(34) model the minimum up time, whereas (35)-(37) correspond to the minimum down time:

$$\sum_{t=1}^{T_{i,0}^{UT}} \left(1 - u_{i,t}\right) = 0 \quad \forall i \in I \,|\, T_{i,0}^{UT} > 0 \tag{32}$$

$$\sum_{t'=t}^{t+UT_i-1} u_{i,t'} \ge UT_i\left(u_{i,t} - u_{i,t-1}\right) \quad \forall i \in I, t \in \left\{T_{i,0}^{UT}+1, T_{i,0}^{UT}+2, \ldots, |T| - UT_i + 1\right\} \tag{33}$$

$$\sum_{t'=t}^{|T|} \left[u_{i,t'} - \left(u_{i,t} - u_{i,t-1}\right)\right] \ge 0 \quad \forall i \in I, t \in \left\{|T| - UT_i + 2, |T| - UT_i + 3, \ldots, |T|\right\} \tag{34}$$

$$\sum_{t=1}^{T_{i,0}^{DT}} u_{i,t} = 0 \quad \forall i \in I \,|\, T_{i,0}^{DT} > 0 \tag{35}$$

$$\sum_{t'=t}^{t+DT_i-1} \left(1 - u_{i,t'}\right) \ge DT_i\left(u_{i,t-1} - u_{i,t}\right) \quad \forall i \in I, t \in \left\{T_{i,0}^{DT}+1, T_{i,0}^{DT}+2, \ldots, |T| - DT_i + 1\right\} \tag{36}$$

$$\sum_{t'=t}^{|T|} \left[1 - u_{i,t'} - \left(u_{i,t-1} - u_{i,t}\right)\right] \ge 0 \quad \forall i \in I, t \in \left\{|T| - DT_i + 2, |T| - DT_i + 3, \ldots, |T|\right\} \tag{37}$$

where $T_{i,0}^{UT} = \min\left\{|T|, \left(UT_i - T_{i,0}^{on}\right) U_{i,0}\right\}$ and $T_{i,0}^{DT} = \min\left\{|T|, \left(DT_i - T_{i,0}^{off}\right)\left(1 - U_{i,0}\right)\right\}, \forall i \in I.$

E. Transmission Network Operation

The characterization of transmission network operation in the pre-contingency and contingency states relies on the SF-based power flow model described in Section II.

For the pre-contingency state, line power losses are cast in (38) in terms of auxiliary variables $\hat{f}_{l,t}$, which are modeled in (39). Moreover, line capacity limits are imposed in (40) and (41).

$$f_{l,t}^{loss} = \frac{G_l}{B_l^2} \hat{f}_{l,t}^2 \quad \forall l \in L, \forall t \in T \tag{38}$$

$$\hat{f}_{l,t} = \sum_{j \in J} SF_{l,j}^{loss} \cdot \left[\sum_{i \in I_j} p_{i,t}^g + ens_{j,t} - P_{j,t}^d - 0.5\left(\sum_{l' \in L | fr(l') = j} f_{l',t}^{loss} + \sum_{l' \in L | to(l') = j} f_{l',t}^{loss}\right)\right] \quad \forall l \in L, \forall t \in T \tag{39}$$

$$\hat{f}_{l,t} + 0.5 f_{l,t}^{loss} \le F_l^{\max} \quad \forall l \in L, \forall t \in T \tag{40}$$

$$-\hat{f}_{l,t} + 0.5 f_{l,t}^{loss} \le F_l^{\max} \quad \forall l \in L, \forall t \in T \tag{41}$$

The need for computing and storing the SF matrix for every contingency state and islanded area is prevented by using fictitious nodal injections to represent out-of-service lines [26], [36], [37]. Bearing in mind that computing the SF matrix involves a matrix inversion (11), the use of fictitious nodal injections is computationally appealing as a single SF matrix is required, namely that associated with the pre-contingency state.

As depicted in Supplementary Material A Fig. SA1, the outage of line l during period t is equivalently modeled by: ① considering the fictitious operation of the line, which is represented by variables $\hat{f}_{l,t}^c$ and $f_{l,t}^{loss,c}$; ② adding at the sending bus a fictitious generation equal to $\hat{f}_{l,t}^c + 0.5 f_{l,t}^{loss,c}$; and ③ adding at the receiving bus a fictitious demand equal to $\hat{f}_{l,t}^c - 0.5 f_{l,t}^{loss,c}$. Additionally, $\hat{f}_{l,t}^c$ for the out-of-service line is not limited by its line capacity.

Compared with the original model wherein the line outage is characterized by explicitly removing the out-of-service line, the proposed model requires: ① the consideration of Kirchhoff's voltage law for the out-of-service line; and ② the incorporation of the fictitious injections in the expressions associated with Kirchhoff's current law at both ends of the out-of-service line. It should be emphasized that the latter modification gives rise to power balance equations wherein the newly added terms cancel out, thereby being identical to those in the original model without the out-of-service line. More specifically, at the sending bus, the fictitious generation $\hat{f}_{l,t}^c + 0.5 f_{l,t}^{loss,c}$ is equal to the outgoing fictitious power flow. Analogously, at the receiving bus, the fictitious demand $\hat{f}_{l,t}^c - 0.5 f_{l,t}^{loss,c}$ is equal to the incoming fictitious power flow. As a result, $\hat{f}_{l,t}^c$ and $f_{l,t}^{loss,c}$ for the out-of-service line are solely used in the corresponding Kirchhoff's voltage law equations, where each variable is expressed in terms of other optimization variables. Hence, such equalities have no impact on the optimization process and can thus be dropped along with the newly added variables $\hat{f}^c_{l,t}$ and $f^{loss,c}_{l,t}$, which yields exactly the same optimization problem as the original model.

Accordingly, (42)-(45) correspond to (38)-(41) for the contingency state, respectively:

$$f^{loss,c}_{l,t}=\frac{G_l}{B_l^2}\left(\hat{f}^c_{l,t}\right)^2 \quad \forall l\in L^c, \forall t\in T \tag{42}$$

$$\begin{aligned}\hat{f}^c_{l,t}=&\sum_{j\in J}SF^{loss}_{l,j}\cdot\Bigg[\sum_{i\in I^c_j}p^{g,c}_{i,t}+ens^c_{j,t}-P^d_{j,t}-\\&0.5\Bigg(\sum_{l'\in L^c|fr(l')=j}f^{loss,c}_{l',t}+\sum_{l'\in L^c|to(l')=j}f^{loss,c}_{l',t}\Bigg)\Bigg]+\\&\sum_{l'\notin L^c}\left(SF^{loss}_{l,fr(l')}\hat{f}^c_{l',t}-SF^{loss}_{l,to(l')}\hat{f}^c_{l',t}\right) \quad \forall l\in L,\forall t\in T\end{aligned} \tag{43}$$

$$\hat{f}^c_{l,t}+0.5f^{loss,c}_{l,t}\le F^{\max}_l \quad \forall l\in L^c,\forall t\in T \tag{44}$$

$$-\hat{f}^c_{l,t}+0.5f^{loss,c}_{l,t}\le F^{\max}_l \quad \forall l\in L^c,\forall t\in T \tag{45}$$

The losses for operational lines are modeled in (42). Expression (43) characterizes auxiliary variables $\hat{f}^c_{l,t}$ for all lines in terms of pre-contingency lossy SFs and nodal injections under contingency. Note that, compared with their pre-contingency counterparts (39), an extra last term is included in (43). Such a term models the effect of the newly added fictitious injections [26]. Moreover, in contrast to the lossless instances in [26], [36], and [37], (43) features two distinctive aspects: ① lossy SFs are used; and ② the power injection at each bus incorporates the loss contributions of the lines connecting that bus, which are modeled by the last two summations within the square brackets. Moreover, as per (44) and (45), line capacities are solely imposed for lines in service.

It should be emphasized that (42)-(45) constitute an original extension of the fictitious-injection-based model presented in [36] and [37], where transmission losses are neglected.

Due to the presence of quadratic expressions (38) and (42) for transmission losses, problem (12)-(45) is a computationally expensive instance of mixed-integer quadratically-constrained programming (MIQCP). In order to leverage the methodological and computational benefits featured by an MILP framework, the quadratic expressions for transmission losses in (38) and (42) are linearized using an effective binary-variable-based piecewise linear approximation. This approximation is based on standard findings of operation research [42], [43] and relevant works in the power system literature [29], [30], where a less accurate piecewise linearization is reported for quadratic line losses. For practical purposes, the piecewise linear approximation is indistinguishable from the quadratic function if enough blocks are used [42]. By a tedious but straightforward calculation, the maximum error of the approximation for a given line l amounts to $\frac{G_l}{4B_l^2}\left(\frac{F^{\max}_l}{|S|}\right)^2$.

As per (38), pre-contingency transmission losses are cast as $f^{loss}_{l,t}=\frac{G_l}{B_l^2}\hat{f}^2_{l,t}$, where $\hat{f}_{l,t}$ can take both positive and negative values. Similar to the piecewise linear approximation described in [29] and [30], the linearization in this paper is equivalently reduced to the positive orthant, i.e., $\frac{G_l}{B_l^2}\left|\hat{f}_{l,t}\right|^2$ is linearized rather than the original $\frac{G_l}{B_l^2}\hat{f}^2_{l,t}$. To that end, each term $\left|\hat{f}_{l,t}\right|$ is discretized into a set of blocks [42], whereas the absolute value function is represented by the sum of two auxiliary non-negative variables $\hat{f}^+_{l,t}$ and $\hat{f}^-_{l,t}$ [43]:

$$f^{loss}_{l,t}=\frac{G_l}{B_l^2}\sum_{s\in S}\zeta_{s,l}\Delta\hat{f}_{s,l,t} \quad \forall l\in L,\forall t\in T \tag{46}$$

$$z_{1,l,t}\frac{F^{\max}_l}{|S|}\le\Delta\hat{f}_{1,l,t}\le\frac{F^{\max}_l}{|S|} \quad \forall l\in L,\forall t\in T \tag{47}$$

$$z_{s,l,t}\frac{F^{\max}_l}{|S|}\le\Delta\hat{f}_{s,l,t}\le z_{s-1,l,t}\frac{F^{\max}_l}{|S|} \quad s\in\{2,3,\dots,|S|-1\},\forall l\in L,\forall t\in T \tag{48}$$

$$0\le\Delta\hat{f}_{|S|,l,t}\le z_{|S|-1,l,t}\frac{F^{\max}_l}{|S|} \quad \forall l\in L,\forall t\in T \tag{49}$$

$$z_{s,l,t}\in\{0,1\} \quad s\in\{1,2,\dots,|S|-1\},\forall l\in L,\forall t\in T \tag{50}$$

$$\sum_{s\in S}\Delta\hat{f}_{s,l,t}=\hat{f}^+_{l,t}+\hat{f}^-_{l,t} \quad \forall l\in L,\forall t\in T \tag{51}$$

$$\hat{f}_{l,t}=\hat{f}^+_{l,t}-\hat{f}^-_{l,t} \quad \forall l\in L,\forall t\in T \tag{52}$$

$$0\le\hat{f}^+_{l,t}\le y_{l,t}F^{\max}_l \quad \forall l\in L,\forall t\in T \tag{53}$$

$$0\le\hat{f}^-_{l,t}\le\left(1-y_{l,t}\right)F^{\max}_l \quad \forall l\in L,\forall t\in T \tag{54}$$

$$y_{l,t}\in\{0,1\} \quad \forall l\in L,\forall t\in T \tag{55}$$

where $\zeta_{s,l}=(2s-1)\frac{F^{\max}_l}{|S|},\forall s\in S,\forall l\in L$.

The linearized version of (38) is formulated in (46). Expressions (47)-(50) model the block discretization, whereas (51)-(55) correspond to the linearization of the absolute value function. It is worth highlighting that, unlike the linear schemes presented in [29] and [30], two sets of extra binary variables, denoted by $z_{s,l,t}$ and $y_{l,t}$, are used to guarantee compliance with two critical requirements: ① the adjacency condition, whereby the blocks used in the discretization should be filled sequentially, which is modeled in (47)-(49) by binary variables $z_{s,l,t}$ based on [42]; and ② the complementarity condition, whereby both auxiliary variables $\hat{f}^+_{l,t}$ and $\hat{f}^-_{l,t}$ cannot be different from 0 simultaneously. According to [42], this is modeled in (53) and (54) through binary variables $y_{l,t}$.

As a consequence, (46)-(55) overcome the issues of the simpler albeit potentially inconsistent linear formulations of [29] and [30], which may lead to impractical solutions featuring the so-called fictitious losses [44].

Analogously, quadratic transmission losses in the contingency state (42) are replaced with mixed-integer linear expressions (56)-(65):

$$f^{loss,c}_{l,t}=\frac{G_l}{B_l^2}\sum_{s\in S}\zeta_{s,l}\Delta\hat{f}^c_{s,l,t} \quad \forall l\in L^c,\forall t\in T \tag{56}$$

$$z_{1,l,t}^{c}\frac{F_{l}^{\max}}{|S|} \le \Delta\hat{f}_{1,l,t}^{c} \le \frac{F_{l}^{\max}}{|S|} \quad \forall l \in L^{c}, \forall t \in T \tag{57}$$

$$z_{s,l,t}^{c}\frac{F_{l}^{\max}}{|S|} \le \Delta\hat{f}_{s,l,t}^{c} \le z_{s-1,l,t}^{c}\frac{F_{l}^{\max}}{|S|}$$
$$s \in \{2,3,\ldots,|S|-1\}, \forall l \in L^{c}, \forall t \in T \tag{58}$$

$$0 \le \Delta\hat{f}_{|S|,l,t}^{c} \le z_{|S|-1,l,t}^{c}\frac{F_{l}^{\max}}{|S|} \quad \forall l \in L^{c}, \forall t \in T \tag{59}$$

$$z_{s,l,t}^{c} \in \{0,1\} \quad s \in \{1,2,\ldots,|S|-1\}, \forall l \in L^{c}, \forall t \in T \tag{60}$$

$$\sum_{s \in S}\Delta\hat{f}_{s,l,t}^{c} = \hat{f}_{l,t}^{+,c} + \hat{f}_{l,t}^{-,c} \quad \forall l \in L^{c}, \forall t \in T \tag{61}$$

$$\hat{f}_{l,t}^{c} = \hat{f}_{l,t}^{+,c} - \hat{f}_{l,t}^{-,c} \quad \forall l \in L^{c}, \forall t \in T \tag{62}$$

$$0 \le \hat{f}_{l,t}^{+,c} \le y_{l,t}^{c}F_{l}^{\max} \quad \forall l \in L^{c}, \forall t \in T \tag{63}$$

$$0 \le \hat{f}_{l,t}^{-,c} \le \left(1 - y_{l,t}^{c}\right)F_{l}^{\max} \quad \forall l \in L^{c}, \forall t \in T \tag{64}$$

$$y_{l,t}^{c} \in \{0,1\} \quad \forall l \in L^{c}, \forall t \in T \tag{65}$$

Similar to the mixed-integer linearization of the pre-contingency transmission losses, binary variables $z_{s,l,t}^{c}$ and $y_{l,t}^{c}$ are used to meet the adjacency and complementarity conditions under contingency, respectively.

F. Practical Implementation

The ultimate goal of the proposed model is to allow power system operators to ex-ante schedule energy and reserves over a multiperiod time horizon while accounting for security. Thus, the tool presented in this paper is suitable for day-ahead market clearing in current co-optimized electricity markets adopting a two-settlement procedure such as those currently implemented across the USA [45]. As a relevant feature, the physical deliverability of spinning reserves is ensured by explicitly modeling the post-contingency operation of power system via (18), (20), (26)-(28), (43)-(45), and (56)-(65). Moreover, it is worth emphasizing that the reliance of the proposed model on MILP is relevant for practical implementation as the state-of-the-art branch-and-cut algorithm is readily available in the form of both commercial and open-source off-the-shelf software. Thus, the proposed model can be incorporated as a routine procedure within the suite of decision-making tools of power system operators.

For large systems, the number of binary variables may be prohibitive. In such cases, an iterative process can be implemented to regain tractability. The process begins with the solution of a relaxed version of the proposed model where binary variables $z_{s,l,t}$, $y_{l,t}$, $z_{s,l,t}^{c}$, and $y_{l,t}^{c}$ are dropped. In case the adjacency or the complementarity conditions are violated, the corresponding binary variables are incorporated into the formulation, and the resulting model is solved. This process continues until the adjacency and the complementarity conditions are all met.

IV. Case Studies

This section examines three case studies based on standard test systems. The first case study analyzes the IEEE 14-bus system, which allows comprehensively illustrating the modeling contributions highlighted in Section I. The second case study, based on the IEEE 118-bus system, is useful to corroborate the effectiveness of the proposed model in terms of solution quality and computational performance. In the third case study, a realistic industry-scale 500-bus system is used to demonstrate the practical applicability of the proposed model. In all cases, a 24-hour time span is examined, the hourly load percentage levels from [46] are considered, and 6-block linearized loss functions are used.

In order to empirically back the main contributions of this paper, the proposed model has been assessed with alternative formulations based on MILP and MIQCP. The MIQCP model (12)-(45) is particularly useful to illustrate the appealing trade-off between solution quality and computational effort struck by the proposed instance of MILP, which comprises (12)-(37), (39)-(41), and (43)-(65).

Simulations have been conducted on a desktop computer equipped with an Intel Core i7 processor clocking at 2.6 GHz with 16 GB of RAM. MATLAB is used for data manipulation and computation of the SF matrix. The MILP and MIQCP instances are respectively solved using OSIXpress 8.14 [47] and Gurobi 11.0.3 [48] both under GAMS. Both solvers are stopped when either a 0.1% optimality tolerance is met or a practical four-hour time limit is reached [10]. Moreover, the running time reported for each instance is the average time over 10 executions.

A. IEEE 14-bus System

This test system consists of 5 generators, 20 transmission lines, and 11 loads. Transmission line capacity limits are set according to [49]. The nodal peak load profiles and generation cost coefficients can be found in the MATPOWER database [50]. All other system parameters can be found in [51]. Supplementary Material A Fig. SA2 depicts the one-line diagram for this system.

1) Benefits of Corrective Actions

The corrective model is firstly assessed with an extended version of the state-of-the-art preventive model [12]. As corrective actions are neglected by the MILP formulation used for assessment, such a model cannot handle generator outages. Thus, for the sake of a fair comparison, three contingency states are considered for both the corrective and the preventive models. Such contingency states are provided in Supplementary Material A Table SAII. Note that, for each value of *k*, line unavailability spans the whole scheduling horizon.

The total costs for both models are depicted in Fig. 1 for the three contingency states under consideration. As expected, the corrective model leads to substantial cost savings ranging between 5.5% and 18.4%. These results are consistent with the preventive model ensuring the feasibility of post-contingency operation without allowing pre-contingency scheduling and dispatch decisions to differ from those under contingency. In other words, the preventive model is equivalent to a more constrained instance of the corrective model, wherein reserves are all set to be 0. On the other hand, the corrective model jointly identifies the optimal pre-contingency generation schedule and post-contingency generation redispatch through the allocation and deployment of reserves.

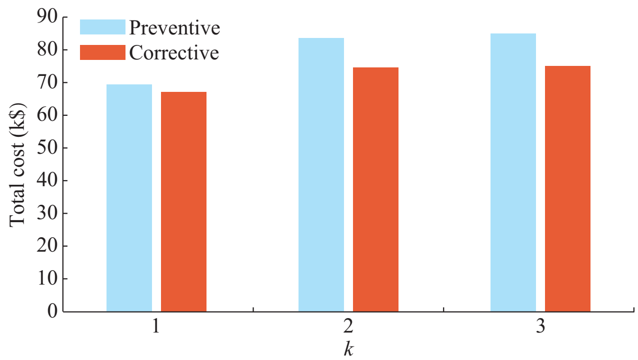

Fig. 1. Total costs for corrective and preventive models for IEEE 14-bus system.

Interestingly, in the corrective model, the total cost for $k=2$ with lines L4 and L6 out of service is higher than that for $k=3$ with L2 also unavailable, as shown in Supplementary Material A Table SAII. Such a cost increase is due to the larger number of transitions between the on and off states, as well as the greater participation of the most expensive generator, namely G5. This result is aligned with the findings of [52], where line switching is suggested as a useful corrective action.

2) Impact of Accuracy of Loss Modeling

This case study is useful for examining the economic and computational impact of the accuracy of loss modeling. To this end, we have also implemented three alternative models with different representations for transmission losses, namely ① lossless model; ② model with linear programming (LP) losses presented in [30]; and ③ model with quadratic losses based on (38) and (42), which gives rise to an MIQCP scheduling problem.

All models have been run for values of k ranging from 0 to 5. Supplementary Material A Table SAIII presents the contingency states resulting from the above-described outage selection procedure. In order to validate the robustness of this procedure, we have solved the proposed model for all possible contingency states for $k=1$ and $k=2$. Remarkably, for such values of k, the solutions corresponding to the contingency states identified by the proposed selection procedure outperform 95.7% and 99.6% of the solutions associated with other possible contingency states, respectively. In other words, the reserves scheduled under the contingency state selected by the procedure allow guarding against the occurrence of almost all other possible contingency states. These results corroborate the ability of the outage selection procedure to identify critical contingency states.

Table I reports the total costs and computational time for the four models under assessment. For a fair comparison with the solutions attained by the model with quadratic losses, the costs reported in Table I for the three other models are not those provided by the corresponding optimization processes, which feature simpler loss characterizations. Rather, as done in [40] and [53], the actual total costs for the solutions to those approximate models are provided. Such actual costs result from solving the MIQCP version with the unit commitment decisions and reserve schedule fixed to the values of the corresponding solution. Note, however, that the computational effort incurred by the calculation of the actual total cost is not accounted for in Table I.

TABLE I
TOTAL COSTS AND COMPUTATIONAL TIME FOR THE IEEE 14-BUS SYSTEM

k	Lossless model		Model with LP losses		Proposed model with MILP losses		Model with quadratic losses	
	Total cost (k$)	Time (s)	Total cost (k$)	Time (s)	Total cost (k$)	Time (s)	Total cost (k$)	Time (s)
0	307.39	0.82	51.53	4.01	51.53	16.24	51.53	47.10
1	67.15	0.12	67.14	1.86	67.14	26.93	67.14	56.16
2	87.18	0.10	87.22	4.09	87.18	72.38	87.18	179.73
3	87.19	0.10	87.22	2.81	87.19	125.03	87.19	137.65
4	87.81	1.10	87.54	9.12	87.54	115.81	87.54	271.94
5	299.43	0.91	88.26	12.17	88.26	119.27	88.26	586.93

In general, as k grows, so does the total cost, whereas the MIQCP model, i.e., the model with quadratic losses, requires the longest computational time. Table I also shows that, compared with the model with quadratic losses, the binary-variable-based approximation strikes a suitable trade-off between computational effectiveness and accuracy, as substantial time savings between 9.17% and 79.68% are achieved at the expense of negligible increases in the total cost below 0.001%.

From Table I, the model with LP losses seems to be a competitive alternative to the proposed model, bearing in mind that the computational time required to achieve solutions with almost identical total costs is between one and two orders of magnitude shorter. However, this appealing performance involves impractical solutions violating the adjacency and/or complementarity conditions described in Section III-E. Thus, unlike the solutions provided by the proposed model, fictitious losses are featured, as illustrated in Supplementary Material A Tables SAIV and SAV.

Supplementary Material A Table SAIV exemplifies the lack of adjacency experienced by the solution provided by the model with LP losses. The results reported in this table correspond to the discretization of the pre-contingency transmission line power loss for line L15 at hour 6 for $k=2$. Note that the use of non-consecutive blocks in the piecewise linearization of the LP model yields fictitious losses exceeding by 25.4% the value identified by the proposed formulation.

Supplementary Material A Table SAV illustrates the complementarity issue featured by the model with LP losses for $k=1$ in the post-contingency state at hour 5. As can be seen, the complementarity condition is violated for lines L2 and L14 when the model with LP loss is used. In spite of their difference being close or even identical to that resulting from the proposed model, the non-zero values of $\hat{f}_{l,5}^{+,c}$ and $\hat{f}_{l,5}^{-,c}$ attained by the model with LP losses give rise to fictitious losses. It is important to highlight that line L14 features this issue throughout the entire scheduling horizon.

This case study is also useful to reveal the drawback of neglecting losses, which is significantly faster albeit potentially leading to load shedding. As shown in Table I, this issue is experienced for $k=0$ and $k=5$, for which the unit commitment and reserve schedule identified by the lossless model cannot meet the demand. This result motivates the practical need for loss-concerned generation scheduling tools such as the proposed model.

The impact of the number of blocks $|S|$ used in the piecewise linearization on solution quality and computational performance has been examined through a sensitivity analysis. Supplementary Material A Table SAVI summarizes the main results for the values of k considered in Table I. Compared with the more accurate and hence computationally costlier instances with 8 and 10 blocks, the instances with 2 and 4 blocks are solved faster, but the solution quality is unacceptable especially in terms of system losses. By contrast, when 6 blocks are used, the total costs and losses are similar to the best possible values, whereas a significantly shorter computational time is required. These results back 6 blocks as the trade-off choice, which is consistent with the findings in [30].

Finally, in order to shed light on the computational challenges associated with the incorporation of losses into CSCUC, this illustrative example has been used to test an extended loss-concerned and multiperiod version of the contingency-constrained approach described in [13], where transmission losses are neglected and a single-period setting is adopted. Unfortunately, even for the less stringent $N-1$ criterion, the branch-and-cut algorithm of OSIXpress fails to identify a single feasible solution for the resulting instance of MILP after 14 hours.

B. IEEE 118-bus System

This case study approximates an electric power system in the Midwest of the USA. This system comprises 54 generators, 186 transmission lines, and 91 loads [50]. The peak load is 4242 MW, while the total generation capacity is 9966.20 MW. Critical components in descending order of severity are generators G40, G29, and G28, located at buses 89, 66, and 65, respectively, and lines L9, L178, and L110.

For this case study, Gurobi fails to find a solution for the MIQCP counterpart within the practical four-hour time limit [10]. Therefore, the performance of the proposed model has been assessed with the two other formulations used in Section IV-A, namely the lossless model and the model with LP losses. Following a procedure similar to that described in Section IV-A, Table II reports the actual total costs and computational time for the lossless model, the model with LP losses, and the proposed model with MILP losses. Moreover, similar to Table I, the computational time presented in Table II does not consider the process of calculating the actual total cost.

TABLE II
TOTAL COSTS AND COMPUTATIONAL TIME FOR IEEE 118-BUS SYSTEM

k	Lossless model		Model with LP losses		Proposed model with MILP losses	
	Total cost (k$)	Time (s)	Total cost (k$)	Time (s)	Total cost (k$)	Time (s)
0	4272.08	11.13	4271.57	2369.76	4271.57	1355.16
1	4293.30	21.62	4283.83	2121.19	4273.44	2691.52
2	4277.00	18.14	4280.97	2164.75	4275.29	3180.87
3	4289.69	24.11	4289.78	1983.37	4286.24	2527.09
4	4311.01	23.64	4310.89	2148.71	4289.98	3943.38
5	4314.45	24.09	4309.42	2167.28	4290.30	3273.47
6	4324.46	24.85	4317.41	2139.36	4296.08	3276.43

Table II shows that the lossless model exhibits the poorest performance in terms of solution quality. Compared with the proposed model, an increase in the total cost of up to 0.66% is featured. Table II also reveals the superiority of the proposed model over the model with LP losses. As can be observed, a maximum 0.49% reduction in the total cost is reached for $k=6$. It is worth pointing out that such high-quality solutions are achieved within practical computational time. Thus, these results substantiate that it is technically and economically appealing to precisely incorporate transmission losses in CSCUC despite the larger computational burden.

C. 500-bus System

In order to assess the scalability of the proposed model, a case study based on a synthetic 500-bus system [50] is also analyzed. This system comprises 90 generators, 597 transmission lines, and 206 loads. From highest to lowest severity, generators G1, G3, and G14 located at buses 9, 17, and 127, respectively, and lines L578, L80, and L205 are identified by the procedure for selecting component outages.

Table III lists the total costs and computational time for values of k up to 6. As can be observed, the total cost moderately rises as the security criterion becomes tighter, whereas the computational time remains within the prescribed limit. These results corroborate the practical applicability of the proposed model.

TABLE III
TOTAL COSTS AND COMPUTATIONAL TIME FOR 500-BUS SYSTEM

k	Total cost (k$)	Time (s)
0	6895.53	8519.97
1	6933.90	8981.43
2	7120.77	12847.86
3	7358.57	12616.64
4	7544.16	12623.51
5	7567.67	12140.30
6	7568.11	12158.23

For the values of k considered in Table III, Supplementary Material A Figs. SA3-SA5 illustrate the evolution of the total cost, transmission losses, and computational time with the number of blocks used in the piecewise linearization. As can be seen in Supplementary Material A Figs. SA3 and SA4, for 6 or fewer blocks, the total cost and especially losses decline abruptly. By contrast, the gain in solution quality attained by considering more blocks stabilizes and does not offset the substantial increase in the computational time (as shown in Supplementary Material A Fig. SA5). Thus, selecting 6 blocks yields the best trade-off between accuracy and computational performance.

V. Conclusion

Within the context of security-constrained electricity markets, this paper proposes a novel corrective $N-k$ SCUC model by jointly considering corrective actions, multiple simultaneous generator and line outages, and transmission network losses. Using an exogenous set of critical components, the corresponding $N-k$ contingency state is explicitly modeled so that reserves can be optimally deployed and delivered across the power system. From a modeling perspective, a major novelty is featured by accounting for pre- and post-contingency transmission losses through a set of lossy SFs and a binary-variable-based piecewise linear approximation. In addition, fictitious injections of active power are used to characterize line outages, thereby requiring the calculation of a single SF matrix.

The proposed model using lossy SFs and fictitious injections is an instance of MILP. The successful numerical experience with three standard benchmarks reveals that the proposed model can effectively obtain high-quality solutions in computational time suitable for current industry practices, and outperform alternative models.

The proposed model has three main limitations. Firstly, a deterministic framework is adopted, whereby the uncertainty in nodal net injections due to the increasing penetration of renewable generation sources is neglected. Secondly, the precise characterization of transmission losses through binary variables yields an instance of MILP that may be computationally challenging. And thirdly, the reliance on a simple and fast outage selection procedure may discard critical contingency states, which biases the resulting generation schedule.

Further work will address such limitations through the adoption of uncertainty-aware approaches based on stochastic programming and robust optimization, the application of iterative algorithms including decomposition techniques and the identification of unnecessary binary variables, and the increase in robustness through alternative outage selection procedures and the joint consideration of several contingency states. Other interesting avenues of research are the incorporation of an $N-1-1$ security criterion, allowing for intermediate adjustments between contingencies, and the consideration of flexibility-enabling technologies such as quick-start units, storage devices, and line switching.

References

[1] California ISO. (2017, Mar.). Generator contingency & RAS modeling – revised straw proposal. [Online]. Available: https://www.caiso.com/Documents/RevisedStrawProposal-GeneratorContingencyRemedialActionSchemeModeling.pdf

[2] M. Panteli and P. Mancarella, "Influence of extreme weather and climate change on the resilience of power systems: impacts and possible mitigation strategies," *Electric Power Systems Research*, vol. 127, pp. 259-270, Oct. 2015.

[3] C. MacIver, K. Bell, and M. Nedd, "An analysis of the August 9th 2019 GB transmission system frequency incident," *Electric Power Systems Research*, vol. 199, p. 107444, Oct. 2021.

[4] N. Sharma, A. Acharya, I. Jacob *et al.*, "Major blackouts of the decade: underlying causes, recommendations and arising challenges," in *Proceedings of the 9th IEEE International Conference on Power Systems*, Kharagpur, India, Dec. 2021, pp. 1-6.

[5] G. Zhang, H. Zhong, Z. Tan *et al.*, "Texas electric power crisis of 2021 warns of a new blackout mechanism," *CSEE Journal of Power and Energy Systems*, vol. 8, no. 1, pp. 1-9, Jan. 2022.

[6] B. Schäfer and G. C. Yalcin, "Dynamical modeling of cascading failures in the Turkish power grid," *Chaos*, vol. 29, no. 9, p. 093134, Sept. 2019.

[7] ENTSO-E. (2021, Jul.). Continental Europe synchronous area separation on 08 January 2021. [Online]. Available: https://eepublicdownloads. azureedge. net/clean-documents/SOC% 20documents/SOC% 20Reports/entso-e_CESysSep_Final_Report_210715.pdf

[8] S. Kumar, A. Pandey, P. Goswami *et al.*, "Analysis of Mumbai grid failure restoration on Oct 12, 2020: challenges and lessons learnt," *IEEE Transactions on Power Systems*, vol. 37, no. 6, pp. 4555-4567, Nov. 2022.

[9] Y. Chen, P. Gribik, and J. Gardner, "Incorporating post zonal reserve deployment transmission constraints into energy and ancillary service co-optimization," *IEEE Transactions on Power Systems*, vol. 29, no. 2, pp. 537-549, Mar. 2014.

[10] Y. Chen, A. Casto, F. Wang *et al.*, "Improving large scale day-ahead security constrained unit commitment performance," *IEEE Transactions on Power Systems*, vol. 31, no. 6, pp. 4732-4743, Nov. 2016.

[11] S. Fliscounakis, P. Panciatici, F. Capitanescu *et al.*, "Contingency ranking with respect to overloads in very large power systems taking into account uncertainty, preventive, and corrective actions," *IEEE Transactions on Power Systems,* vol. 28, no. 4, pp. 4909-4917, Nov. 2013.

[12] G. Gutiérrez-Alcaraz, B. Díaz-López, J. M. Arroyo *et al.*, "Large-scale preventive security-constrained unit commitment considering $N-k$ line outages and transmission losses," *IEEE Transactions on Power Systems*, vol. 37, no. 3, pp. 2032-2041, May 2022.

[13] J. M. Arroyo and F. D. Galiana, "Energy and reserve pricing in security and network-constrained electricity markets," *IEEE Transactions on Power Systems*, vol. 20, no. 2, pp. 634-643, May 2005.

[14] A. Street, A. Moreira, and J. M. Arroyo, "Energy and reserve scheduling under a joint generation and transmission security criterion: an adjustable robust optimization approach," *IEEE Transactions on Power Systems*, vol. 29, no. 1, pp. 3-14, Jan. 2014.

[15] F. Bouffard, F. D. Galiana, and A. J. Conejo, "Market-clearing with stochastic security – Part I: formulation," *IEEE Transactions on Power Systems*, vol. 20, no. 4, pp. 1818-1826, Nov. 2005.

[16] F. Bouffard, F. D. Galiana, and A. J. Conejo, "Market-clearing with stochastic security – Part II: case studies," *IEEE Transactions on Power Systems*, vol. 20, no. 4, pp. 1827-1835, Nov. 2005.

[17] E. Karangelos and F. Bouffard, "Towards full integration of demand-side resources in joint forward energy/reserve electricity markets," *IEEE Transactions on Power Systems*, vol. 27, no. 1, pp. 280-289, Feb. 2012.

[18] Q. Wang, J.-P. Watson, and Y. Guan, "Two-stage robust optimization for *N-k* contingency-constrained unit commitment," *IEEE Transactions on Power Systems*, vol. 28, no. 3, pp. 2366-2375, Aug. 2013.

[19] R. L.-Y. Chen, N. Fan, A. Pinar *et al.*, "Contingency-constrained unit commitment with post-contingency corrective recourse," *Annals of Operations Research*, vol. 249, no. 1-2, pp. 381-407, Feb. 2017.

[20] Z. Guo, R. L.-Y. Chen, N. Fan *et al.*, "Contingency-constrained unit commitment with intervening time for system adjustments," *IEEE Transactions on Power Systems*, vol. 32, no. 4, pp. 3049-3059, Jul. 2017.

[21] B. Hu and L. Wu, "Robust SCUC considering continuous/discrete uncertainties and quick-start units: a two-stage robust optimization with mixed-integer recourse," *IEEE Transactions on Power Systems*, vol. 31, no. 2, pp. 1407-1419, Mar. 2016.

[22] N. G. Cobos, J. M. Arroyo, and A. Street, "Least-cost reserve offer deliverability in day-ahead generation scheduling under wind uncertainty and generation and network outages," *IEEE Transactions on Smart Grid*, vol. 9, no. 4, pp. 3430-3442, Jul. 2018.

[23] K. Sundar, H. Nagarajan, L. Roald *et al.*, "Chance-constrained unit commitment with $N-1$ security and wind uncertainty," *IEEE Transactions on Control of Network Systems*, vol. 6, no. 3, pp. 1062-1074, Sept. 2019.

[24] Y. Chen, Z. Zhang, Z. Liu *et al.*, "Robust $N-k$ CCUC model considering the fault outage probability of units and transmission lines," *IET Generation, Transmission & Distribution*, vol. 13, no. 17, pp. 3782-3791, Sept. 2019.

[25] D. A. Z. Vazquez, J. L. R. Duarte, N. Fan *et al.*, "$N-1-1$ contingency-constrained unit commitment with renewable integration and corrective actions," *Annals of Operations Research*, vol. 316, no. 1, pp. 493-511, Sept. 2022.

[26] A. J. Wood, B. F. Wollenberg, and G. B. Sheblé, *Power Generation, Operation, and Control*, 3rd ed. Hoboken: John Wiley & Sons, 2014.

[27] S. Zhang and K. W. Hedman, "A computational comparison of PTDF-based and phase-angle-based formulations of network constraints in distributed unit commitment," *Energy Systems*, vol. 14, no. 2, pp. 514-540, May 2023.

[28] Z. Bao, Y. Wan, Z. Hu *et al.*, "DC-based security constraints formulation: a perspective of primal-dual interior point method," *Electric Power Systems Research*, vol. 228, p. 110058, Mar. 2024.

[29] A. L. Motto, F. D. Galiana, A. J. Conejo *et al.*, "Network-constrained multiperiod auction for a pool-based electricity market," *IEEE Transactions on Power Systems*, vol. 17, no. 3, pp. 646-653, Aug. 2002.

[30] H. Zhang, V. Vittal, G. T. Heydt *et al.*, "A mixed-integer linear programming approach for multi-stage security-constrained transmission expansion planning," *IEEE Transactions on Power Systems*, vol. 27, no. 2, pp. 1125-1133, May 2012.

[31] E. Litvinov, T. Zheng, G. Rosenwald *et al.*, "Marginal loss modeling in LMP calculation," *IEEE Transactions on Power Systems*, vol. 19, no. 3, pp. 880-888, May 2004.

[32] M. Caramanis, E. Ntakou, W. W. Hogan *et al.*, "Co-optimization of power and reserves in dynamic T&D power markets with nondispatchable renewable generation and distributed energy resources," *Proceedings of the IEEE*, vol. 104, no. 4, pp. 807-836, Apr. 2016.

[33] B. Eldridge, R. O'Neill, and A. Castillo, "An improved method for the DCOPF with losses," *IEEE Transactions on Power Systems*, vol. 33, no. 4, pp. 3779-3788, Jul. 2018.

[34] New York Independent System Operator. (2024, Oct.). Manual 11: day-ahead scheduling manual (version 9.1). [Online]. Available: https://www.nyiso. com/documents/20142/2923301/dayahd_schd_mnl. pdf/0024bc71-4dd9-fa80-a816-f9f3e26ea53a

[35] Y. Fu and Z. Li, "A direct calculation of shift factors under network islanding," *IEEE Transactions on Power Systems*, vol. 30, no. 3, pp. 1550-1551, May 2015.

[36] P. J. Martínez-Lacañina, J. L. Martínez-Ramos, A. de la Villa-Jaén *et al.*, "DC corrective optimal power flow based on generator and branch outages modelled as fictitious nodal injections," *IET Generation, Transmission & Distribution*, vol. 8, no. 3, pp. 401-409, Mar. 2014.

[37] P. J. Martínez-Lacañina, A. M. Marcolini, and J. L. Martínez-Ramos, "DCOPF contingency analysis including phase shifting transformers," in *Proceedings of the 18th Power Systems Computation Conference*, Wroclaw, Poland, Aug. 2014, pp. 1-7.

[38] K. Purchala, L. Meeus, D. van Dommelen *et al.*, "Usefulness of DC power flow for active power flow analysis," in *Proceedings of the IEEE PES General Meeting*, San Francisco, USA, Jun. 2005, pp. 1-6.

[39] F. Bouffard, F. D. Galiana, and J. M. Arroyo, "Umbrella contingencies in security-constrained optimal power flow," in *Proceedings of the 15th Power Systems Computation Conference*, Liège, Belgium, Aug. 2005, pp. 1-7.

[40] M. Carrión and J. M. Arroyo, "A computationally efficient mixed-integer linear formulation for the thermal unit commitment problem," *IEEE Transactions on Power Systems*, vol. 21, no. 3, pp. 1371-1378, Aug. 2006.

[41] D. A. Tejada-Arango, S. Lumbreras, P. Sánchez-Martín *et al.*, "Which unit-commitment formulation is best? A comparison framework," *IEEE Transactions on Power Systems*, vol. 35, no. 4, pp. 2926-2936, Jul. 2020.

[42] S. P. Bradley, A. C. Hax, and T. L. Magnanti, *Applied Mathematical Programming*. Reading: Addison-Wesley, 1977.

[43] D. Bertsimas and J. N. Tsitsiklis, *Introduction to Linear Optimization*. Belmont: Athena Scientific, 1997.

[44] O. W. Akinbode and K. W. Hedman, "Fictitious losses in the DCOPF with a piecewise linear approximation of losses," in *Proceedings of the IEEE PES General Meeting*, Vancouver, Canada, Jul. 2013, pp. 1-6.

[45] B. F. Hobbs and S. S. Oren, "Three waves of U.S. reforms: following the path of wholesale electricity market restructuring," *IEEE Power & Energy Magazine*, vol. 17, no. 1, pp. 73-81, Jan.-Feb. 2019.

[46] C. Grigg, P. Wong, P. Albrecht *et al.*, "The IEEE Reliability Test System – 1996: a report prepared by the Reliability Test System Task Force of the Application of Probability Methods Subcommittee," *IEEE Transactions on Power Systems*, vol. 14, no. 3, pp. 1010-1020, Aug. 1999.

[47] FICO. (2025, Oct.). Xpress optimization suite. [Online]. Available: https://www.fico.com/

[48] Gurobi Optimization. (2025, Oct.). Gurobi optimizer reference manual. [Online]. Available: https://www.gurobi.com

[49] A. Lotfjou, M. Shahidehpour, Y. Fu *et al.*, "Security-constrained unit commitment with AC/DC transmission systems," *IEEE Transactions on Power Systems*, vol. 25, no. 1, pp. 531-542, Feb. 2010.

[50] MATPOWER. (2025, Oct.). MATPOWER reference manual. [Online]. Available: https://matpower.org

[51] S. Ramírez-López, G. Gutiérrez-Alcaraz, J. M. Arroyo *et al*. (2025, Oct.). Corrective $N-k$ security-constrained unit commitment using lossy shift factors and fictitious injections. [Online]. Available: https://ieee-dataport.org/documents/cscus

[52] R. Saavedra, A. Street, and J. M. Arroyo, "Day-ahead contingency-constrained unit commitment with co-optimized post-contingency transmission switching," *IEEE Transactions on Power Systems,* vol. 35, no. 6, pp. 4408-4420, Nov. 2020.

[53] W. R. Faria, G. Muñoz-Delgado, J. M. Arroyo *et al.,* "Accelerated Benders decomposition for enhanced co-optimized T&D system planning," *IEEE Transactions on Power Systems*, vol. 40, no. 3, pp. 2297-2309, May 2025.

Sergio Ramírez-López received the B.S. and M.Sc. degrees from the Instituto Tecnológico de Morelia (ITM), Morelia, Mexico, in 2021 and 2023, respectively. He is currently pursuing the Ph.D. degree in Programa de Graduados e Investigación en Ingeniería Eléctrica (PGIIE), Tecnológico Nacional de México/ITM, Morelia, Mexico. Since 2023, he has been with the Centro Nacional de Control de Energía (CENACE), Mexico City, Mexico. His research interests include electricity market, planning, and optimization.

Guillermo Gutiérrez-Alcaraz received the B. S. and M. Sc. degrees from the Instituto Tecnológico de Morelia (ITM), Morelia, Mexico, in 1994 and 1996, respectively, and the Ph.D. degree from Iowa State University, Ames, USA, in 2009. He is currently a Full Professor of electrical engineering with the PGIIE, Tecnológico Nacional de México/ITM, Morelia, Mexico. His research interests include operation, planning, and economics of power and distribution systems.

José M. Arroyo received the Ingeniero Industrial degree from the Universidad de Málaga, Málaga, Spain, in 1995, and the Ph.D. degree in power system operation planning from the Universidad de Castilla-La Mancha, Ciudad Real, Spain, in 2000. From June 2003 to July 2004, he held a Richard H. Tomlinson Postdoctoral Fellowship with the Department of Electrical and Computer Engineering, McGill University, Montréal, Canada. He is currently a Full Professor of electrical engineering with the Universidad de Castilla-La Mancha. His research interests include operation, planning, and economics of power system, as well as optimization.

Víctor H. Hinojosa received the Electrical Engineer degree from Escuela Politécnica Nacional, Quito, Ecuador, in 2000, and the Ph.D. degree in electrical engineering from Universidad Nacional de San Juan, San Juan, Argentina, in 2007. He is currently a Full Professor with the Department of Electrical Engineering, Universidad Técnica Federico Santa María, Valparaíso, Chile. His research interests include power system stability, planning, operation, optimization, and stochastic programming.